GLOBAL BIOGEOCHEMICAL CYCLES, VOL. 22, GB3028, doi:10.1029/2007GB003122, 2008

Climate controls on the variability of fires in the tropics and subtropics

Guido R. van der Werf,[1] James T. Randerson,[2] Louis Giglio,[3] Nadine Gobron,[4] and A. J. Dolman[1]

Received 12 October 2007; revised 15 May 2008; accepted 28 May 2008; published 5 September 2008.

[1] In the tropics and subtropics, most fires are set by humans for a wide range of purposes. The total amount of burned area and fire emissions reflects a complex interaction between climate, human activities, and ecosystem processes. Here we used satellite-derived data sets of active fire detections, burned area, precipitation, and the fraction of absorbed photosynthetically active radiation (fAPAR) during 1998–2006 to investigate this interaction. The total number of active fire detections and burned area was highest in areas that had intermediate levels of both net primary production (NPP; 500–1000 g C m^{-2} $year^{-1}$) and precipitation (1000–2000 mm $year^{-1}$), with limits imposed by the length of the fire season in wetter ecosystems and by fuel availability in drier ecosystems. For wet tropical forest ecosystems we developed a metric called the fire-driven deforestation potential (FDP) that integrated information about the length and intensity of the dry season. FDP partly explained the spatial and interannual pattern of fire-driven deforestation across tropical forest regions. This climate-fire link in combination with higher precipitation rates in the interior of the Amazon suggests that a negative feedback on fire-driven deforestation may exist as the deforestation front moves inward. In Africa, compared to the Amazon, a smaller fraction of the tropical forest area had FDP values sufficiently low to prevent fire use. Tropical forests in mainland Asia were highly vulnerable to fire, whereas forest areas in equatorial Asia had, on average, the lowest FDP values. FDP and active fire detections substantially increased in forests of equatorial Asia, however, during El Niño periods. In contrast to these wet ecosystems we found a positive relationship between precipitation, fAPAR, NPP, and active fire detections in arid ecosystems. This relationship was strongest in northern Australia and arid regions in Africa. Highest levels of fire activity were observed in savanna ecosystems that were limited neither by fuel nor by the length of the fire season. However, relations between annual precipitation or drought extent and active fire detections were often poor here, hinting at the important role of other factors, including land managers, in controlling spatial and temporal variability of fire.

Citation: van der Werf, G. R., J. T. Randerson, L. Giglio, N. Gobron, and A. J. Dolman (2008), Climate controls on the variability of fires in the tropics and subtropics, *Global Biogeochem. Cycles*, *22*, GB3028, doi:10.1029/2007GB003122.

1. Introduction

[2] In the tropics and subtropics, fire is used for several purposes including the clearing of forest for pasture or agriculture [*Goldammer*, 1990; *Cochrane*, 2003], for nutrient cycling, pest control, and grassland maintenance in savanna ecosystems [*Scholes and Archer*, 1997], and for the removal of agricultural waste [*Yevich and Logan*, 2003]. The only areas without fires are deserts where fuels are not available and in equatorial tropical forests where precipitation is high year-round. Savanna ecosystems with their alternating wet and dry seasons when fuels respectively build-up and dry out provide ideal fire conditions and observations of fire from space have shown that these ecosystems have the highest fire frequencies [*Cahoon et al.*, 1992; *Barbosa et al.*, 1999; *Stroppiana et al.*, 2000].

[3] Fire dynamics in deforestation areas of tropical forests have received considerable attention because of, including the large impact of fire on regional biodiversity [*Phillips*, 1997; *Curran et al.*, 2004] and because emissions from these fires are an important driver of climate change

[1]Department of Hydrology and Geo-Environmental Sciences, Faculty of Earth and Life Sciences, VU University Amsterdam, Amsterdam, Netherlands.
[2]Department of Earth System Science, University of California, Irvine, California, USA.
[3]Science Systems and Applications, Inc., NASA Goddard Space Flight Center, Greenbelt, Maryland, USA.
[4]Global Environmental Monitoring Unit, Institute for Environment and Sustainability, European Commission Joint Research Center, Ispra, Italy.

0886-6236/08/2007GB003122$12.00

[*Forster et al.*, 2007]. Deforestation is a human-driven process, and deforestation rates are partly dependent on political and economic incentives [*Murdiyarso et al.*, 2004; *Morton et al.*, 2006]. Climate, however, may provide additional constraints because the use of fire in the land clearing process is more effective when fuels dry out for longer periods. Emissions in deforestation areas are therefore usually higher in drought years [*Siegert et al.*, 2001; *Page et al.*, 2002; *Nepstad et al.*, 2004; *van der Werf et al.*, 2004; *Randerson et al.*, 2005] and the use of fire may increase in the future as a result of regional and global climate change [*Hoffmann et al.*, 2003]. Once burned, fragmentation and partial loss of canopy cover allow for a more rapid drying of fuels. This initiates a positive feedback loop that may increase fire activity in tropical forests [*Cochrane et al.*, 1999; *Nepstad et al.*, 1999].

[4] In most savanna ecosystems, the length of the dry season is not a limiting factor for fire. The amount of fuel is much lower than in forested regions. Fires here primarily consume herbaceous vegetation and thus fuel loads depend on the productivity of the preceding wet season. In principle, higher precipitation rates allow for higher rates of net primary production (NPP) and biomass at the onset of the dry season [*Griffin et al.*, 1983]. In Kruger National Park, *van Wilgen et al.* [2000] observed a strong positive correlation between precipitation rates during the wet season and fire activity during the following dry season. *Spessa et al.* [2005] and *Randerson et al.* [2005] found the same positive precipitation - fire activity relationship in northern Australia using different satellite data sets.

[5] Besides precipitation, grazing and land use also influence fuel loads so the precipitation–fire relation may not be uniform. Grazing may lower the amount of fuel and the intensity of fires, allowing for woody encroachment which would not occur with more intense fires [*van Langevelde et al.*, 2003]. These interactions may influence the relationship between climate and fire activity. In the absence of fire, most current savanna regions would have a vastly different composition with substantial increases in tree cover [*Bond et al.*, 2005].

[6] Regional studies like the ones mentioned above have convincingly highlighted the important role of climate in shaping spatial and interannual variability in fire activity. A global analysis of the tropics and subtropics that systematically examines the sensitivity of fire activity across moisture and productivity gradients is now feasible with almost 10 years of satellite-derived fire activity and precipitation from the Tropical Rainfall Measuring Mission (TRMM) satellite.

[7] Here we investigate relations between climate, NPP, and fire activity in the global tropics and subtropics. We used observations of fires derived from TRMM Visible and Infrared Scanner (TRMM-VIRS) [*Giglio et al.*, 2003] and burned area derived from the Moderate Resolution Imaging Spectroradiometer (MODIS) [*Giglio et al.*, 2006]. We also used TRMM satellite retrieved precipitation rates, and Sea-viewing Wide Field-of-view Sensor (SeaWiFS) fraction of absorbed photosynthetically active radiation (fAPAR) as input to the Carnegie-Ames-Stanford-Approach (CASA) biogeochemical model to estimate NPP. We show fire activity was highest in ecosystems with intermediate levels of productivity and that fires limited by fuel availability in arid regions and by the length of the dry season in moist regions. We also show how climate partly regulated the amount of burning in tropical forests with important implications for future deforestation rates. Our quantitative assessment of the role of climate in shaping spatial and temporal variability in fire activity may be beneficial for further improving and testing fire modules in dynamic global vegetation models (DGVMs) aiming to predict future fire patterns.

2. Data Sets and Methods

[8] For our analysis we used several data streams from sensors on-board the TRMM satellite, which has an orbit inclined at 35° and a spatial coverage between 38°N and 38°S [*Kummerow et al.*, 1998]. The orbital properties of TRMM were designed to allow for a progressing overpass time, spanning over one complete diurnal cycle within a month. This allows for a comprehensive assessment of rainfall and fire activity, both of which show pronounced diurnal cycles [*Prins and Menzel*, 1992; *Negri et al.*, 2002; *Giglio*, 2007]. The platform carries several instruments, including the Precipitation Radar (PR) and TRMM Microwave Imager (TMI) that were primarily designed to study rainfall [*Kummerow et al.*, 1998], and the Visible and Infrared Scanner (VIRS) that is used to observe fires [*Giglio et al.*, 2003] in addition to its use for other purposes. We used fAPAR from SeaWiFS on the SeaStar satellite to estimate NPP. TRMM was launched in November 1997 and SeaWiFS in August 1997, and both satellites are still in operation. We used data from January 1998–November 2007, but focused on the 1998–2006 period for those analyses where annual data was needed (e.g., trends in fire activity). Analysis of burned area was confined to the 2001–2006 period because of the availability of MODIS observations. Tropical forest extent was based on the IGBP land cover classification scheme using the MODIS MOD12Q1 land cover type data set for 2001 [*Friedl et al.*, 2002].

2.1. Active Fire Detections

[9] Active fire detections are pixels where a fire was observed during the satellite overpass. Most algorithms to detect fires are based on the strong radiance from fires in the mid-infrared [*Dozier*, 1981]. Active fire products have been developed for several sensors including the Advanced Very High-Resolution Radiometer (AVHRR), Along Track Scanning Radiometer (ATSR), MODIS, and VIRS. Here we used the TRMM-VIRS product that includes corrections for missing observations due to cloud cover [*Giglio et al.*, 2003]. TRMM-VIRS active fire detections are available on a monthly time step with a $0.5° \times 0.5°$ spatial resolution from http://daac.gsfc.nasa.gov/precipitation/trmmVirsFire.shtml and shown in Figure 1a.

2.2. Burned Area

[10] Active fire detections indicate the presence of fire at the time of overpass, but these detections give no direct information about fire size. Although active fires are useful

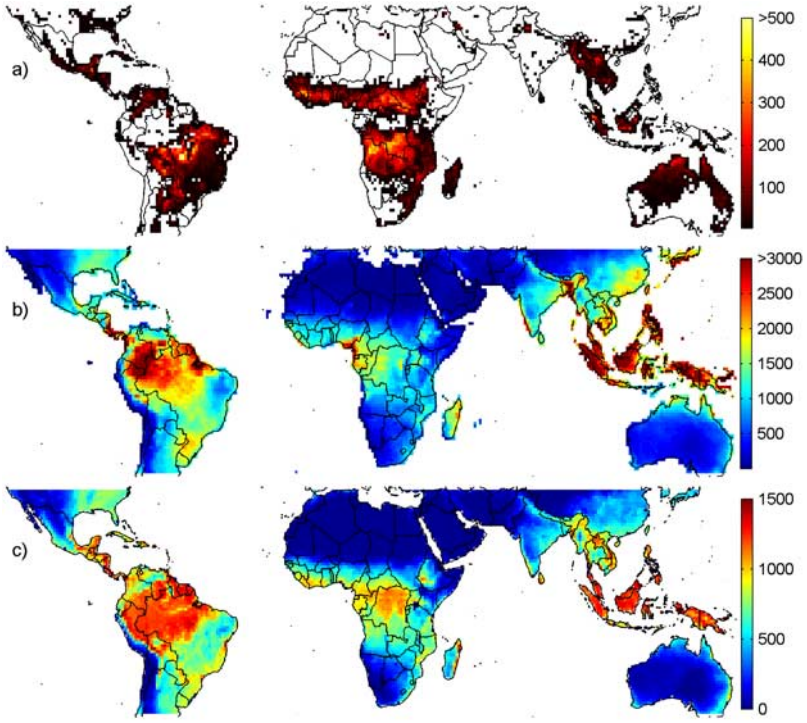

Figure 1. (a) TRMM-VIRS active fire detections (year^{-1}, color scale capped at 500 detections year^{-1}), (b) TRMM-derived precipitation rates (mm year^{-1}, capped at 3000 mm year^{-1}), and (c) net primary production (g C m^{-2} year^{-1}) based on SeaWiFS fAPAR. Fire data were summed, and precipitation and NPP were averaged to a 1° × 1° spatial resolution. All panels show the mean over 1998–2006.

to detect spatial and temporal variability in fire activity, information on burned area is necessary to estimate the spatial extent. Two global burned area data sets exist for the year 2000 (GBA2000 described by *Grégoire et al.* [2003] and GLOBSCAR described by *Tansey et al.* [2004]). Multi-year products based on MODIS [*Roy et al.*, 2005] and SPOT-VGT [*Tansey et al.*, 2008] recently have become available. Here we used data from the global burned area product developed by *Giglio et al.* [2006]. This product relates Terra MODIS fire hot spots to 500 meter Terra MODIS burned area for selected regions, using ancillary data on vegetation continuous fields and the "cluster" size of the hot spots. A region-specific "burned area per active fire detected" scalar is derived as a function of these ancillary data, and extrapolated in time and space to estimate burned area during the MODIS era (starting in 2001) [*Giglio et al.*, 2006]. For clarity, we will use the term burned fraction, which is the fraction of the total area of a grid cell that burned during a given time interval.

2.3. Precipitation

[11] We used the 3B43 time series from TRMM that is based on accumulations of the direct TRMM measurements from both PR and TMI sensors in combination with global gridded rain gauge data. The time series has a monthly time step and a 0.25° × 0.25° spatial resolution [*Huffman et al.*, 1995]. A map with mean annual precipitation (MAP) is shown in Figure 1b.

2.4. fAPAR and NPP

[12] To estimate the fraction of photosynthetically active radiation that is absorbed by plant canopies (fAPAR), we used the SeaWiFS-derived product developed by *Gobron et al.* [2002]. This product uses information from the blue spectral band, which is sensitive to the aerosol loading in the atmosphere, to account for atmospheric effects. The algorithm follows two steps: (1) the spectral bidirectional reflectance factors measured in the red and near-infrared are first rectified for atmospheric contamination using the blue band and adjusted to account for angular effects, and (2) the rectified red and near-infrared bands are then combined to derive fAPAR [*Gobron et al.*, 2006].

[13] For NPP we used a submodule from the CASA biogeochemical model [*Potter et al.*, 1993]. NPP was calculated for each grid cell and month as the product of photosynthetically active radiation (PAR), fAPAR, and a light use efficiency (LUE) that depended locally on temperature and moisture [*Field et al.*, 1998]. PAR was derived from *Bishop and Rossow* [1991] and we used GISTEMP temperature anomalies [*Hansen et al.*, 1999] in combination with the CRU 1961–1990 temperature climatology [*New et al.*, 1999] and TRMM precipitation as data sources to calculate the moisture and temperature controls on the LUE. In our analysis we used a maximum unstressed LUE of 0.5 g C/MJ PAR that was derived from a comparison of modeled and observed NPP [*van der Werf et al.*, 2006]. In Figure 1c a map of mean annual NPP is shown. Mean annual

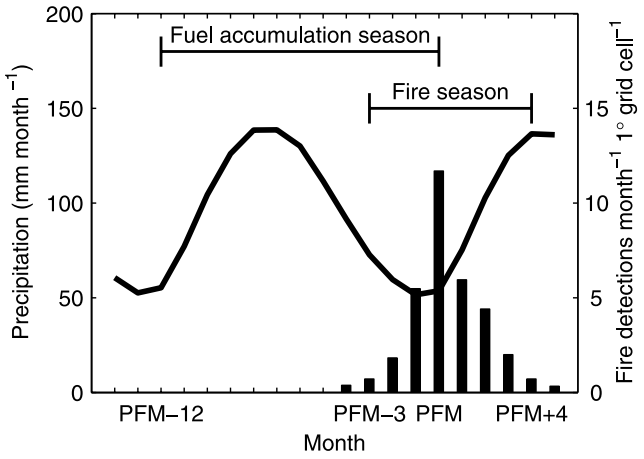

Figure 2. Mean monthly precipitation rates and active fire detections for all grid cells where fire activity was observed. The fire season is defined here as the 8-month period starting 3 months before and ending 4 months after the peak fire month (PFM). The 13-month period preceding and including the peak fire month was used to estimate precipitation levels during the period when herbaceous fuels typically accumulate.

NPP was 40 Pg C year^{-1} for our study region (between 38°N and 38°S).

2.5. Fire-Climate Metrics

[14] Our main objective was to determine the role of climatic controls on spatial and interannual variability in fire activity. For this, fire activity was quantified as the total number of active fire detections or the burned fraction during each fire season. For each grid cell, we defined the fire season as the period starting 3 months before and ending 4 months after the average peak fire month (Figure 2). In most areas fires were confined to a seasonal interval that was considerably shorter than the 8 month fire season we defined here. Thus, over 98% of all TRMM active fires were included in our analysis. The remaining active fire detections were associated with volcanoes, gas flares, and fires burning outside the regular fire season. In Australia, where interannual variability in the peak fire month is relatively large, our approach still captured 94% of the fire detections. We defined the peak fire month as the month with the maximum number of active fire detections over 9 annual fire cycles. We defined a fuel accumulation period as the 13 month period starting 12 months before the average peak fire month. We chose this period to include most of the precipitation available for the growth of annual (herbaceous) plant functional types during the preceding wet season (Figure 2).

[15] We defined a fire-driven deforestation potential (FDP) scalar to investigate the role of drought on fire activity in tropical forests. The FDP scalar combines information about both the length and the intensity of the dry season:

$$FDP_{x,y,t} = \sqrt{\left(\#DM_{x,y,t}/8\right) \times \left(1 - \left(PPT_{DM_{x,y,t}}/100\right)\right)} \quad (1)$$

where #DM is the number of dry months within the 8 month fire season. Dry months were defined as a month with precipitation (PPT) below 100 mm month^{-1} [*Phillips et al.*, 1994; *Saleska et al.*, 2003]. PPT_{DM} represents the mean precipitation during these dry months. This scalar was calculated for each grid cell (x,y) and fire season (t) and yielded a value that was 1 for grid cells with 8 months with zero precipitation, and 0 when precipitation never dropped below 100 mm month^{-1} during the fire season. For the tropical forest grid cells that did not have any active fire observations to define a peak fire month, we extrapolated the peak fire month from neighboring grid cells, taking into account shifts in PPT expected near the equator.

3. Results

[16] In deforestation areas within Southeast Asia and the Amazon, fire activity increased during dry years (Figure 3a, areas in red with a positive correlation between FDP and active fire detections), whereas in arid ecosystems, including the Sahel, the Kalahari Desert in southern Africa, and northern Australia, fire activity increased during wet years (Figure 3b, areas in red with a positive correlation between precipitation rates during the fuel accumulation season and active fire detections). In Figure 3c these two different responses are summarized for different p-levels, areas in red are grid cells where FDP and fire activity were positively correlated, while areas in blue are grid cells where precipitation during the growing season and fire activity were positively correlated. Areas having a negative or positive relation between fire and both FDP and PPT during the growing season were assigned the limiting factor that resulted in the lowest p-value.

[17] The difference in response to drought is shown in more detail for a wet (southern Borneo) and an arid (northwest Australia) ecosystem in Figure 4. Fire activity in wet ecosystems was limited by the length of the dry season, while fire activity in arid ecosystems was limited by the amount of precipitation during the wet season, which partly governed fAPAR and the amount of fuel available to burn (Figure 4c).

[18] Areas receiving about 1000 mm year^{-1} MAP were neither limited by fuel nor by the length of the dry season, but there was no clear MAP threshold separating the two limiting factors. In wet ecosystems where interannual variability in FDP explained more than 50% of the variance in interannual fire activity the 10th percentile, median, and 90th percentile MAP values were 881, 1564, and 2717 mm year^{-1}. In arid ecosystems where IAV in growing season precipitation was a better predictor these MAP values were 408, 658, and 1377 mm year^{-1}, respectively. Maximum fire activity occurred at intermediate levels of precipitation and NPP (Figures 5 and 6). Below we further describe results for deforestation regions, ecosystems with intermediate productivity, and arid ecosystems.

3.1. Tropical Forest Ecosystems

[19] In southern Borneo, we found a strong relationship between fire and the length and intensity of the dry season as represented by FDP (Figures 3a and 4a). FDP and fire activity were also positively correlated in most of the arc of deforestation in the Amazon (the south-eastern edge of the

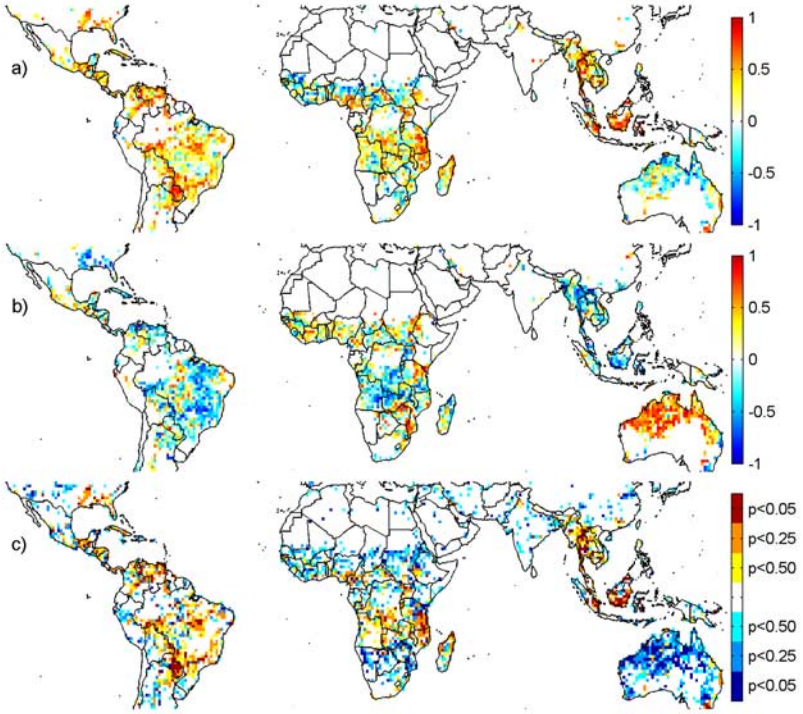

Figure 3. (a) Correlation between annual FDP and the sum of active fire detections during each fire season, showing positive correlations in deforestation areas (Central and South America, southeast Asia) and other regions with high biomass loads (e.g., wooded areas in Africa south of the Congo basin). (b) Correlation between cumulative precipitation over the fuel accumulation season (defined in Figure 2 as the wet season preceding the fire season) and active fire detections during the fire season showing positive correlations in fuel-limited ecosystems, most notably northern Australia. (c) *p*-values for grid cells showing a positive relation between FDP and active fire detections during the fire season (in red) and for grid cells showing a positive relation between cumulative precipitation over the fuel accumulation season and active fire detections during the fire season (in blue). Note that red grid cells in Figure 3b correspond to blue grid cells in Figure 3c.

Amazon where most deforestation takes place) and in Africa, but to a lesser degree than in Borneo.

[20] The mean annual FDP scalar varied substantially within the tropical forest biome (Figure 7a). In tropical America FDP values were high in the arc of deforestation (Figure 1a). Further into the interior FDP values were lower indicating that future fire use may not be as effective or prevalent as it is at the current deforestation front. A similar gradient was observed in Africa, but the total area with low FDP values was smaller, and areas having high precipitation year-round were limited as compared with the Amazon (Table 1). In Southeast Asia, all tropical forests on the mainland had high FDP values whereas the tropical forests areas closer to the equator (Malaysia, Indonesia, Papua New Guinea [PNG]) had low FDP values. Exceptions occurred on the island of Java and the southern part of PNG; these regions experienced an extended dry season annually. Asia had the highest area (both actual area and percentage) of forest with FDP values below 0.3 suggesting that from a climate perspective these forests may be less vulnerable than those in America or Africa (Table 1). Nevertheless, even in low FDP regions of Asia fires were detected (Figure 1a).

[21] The maximum FDP over the 1998–2006 period (Figure 7b) had a similar pattern as the mean FDP (Figure 7a), except for the north-eastern Amazon and equatorial Asia. These regions are influenced by interannual variations in weather patterns related to the El Niño-Southern Oscillation (ENSO) [*Ropelewski and Halpert*, 1987]. This variability is most apparent from Figure 7c, where the FDP standard deviation over 1998–2006 is shown. One implication of this variability is that although southern Borneo had a low mean annual FDP indicating that climate typically limits human use of fire, during El Niño years the region may be as vulnerable to fire as fire-prone regions in the arc of deforestation in Brazil.

3.2. Ecosystems With Intermediate Productivity

[22] In all regions, fire activity peaked between 1000 and 2000 mm year^{-1} of annual precipitation, or 500–1000 g C m^{-2} year^{-1} of annual NPP. In Africa, the peak was more clearly defined and fire activity decreased when precipitation exceeded 1500 mm year^{-1} (Figures 5 and 6). These areas correspond mostly to productive savannas, but also include some forests in Africa and South America (Figure 1). Within these "optimal" precipitation or NPP

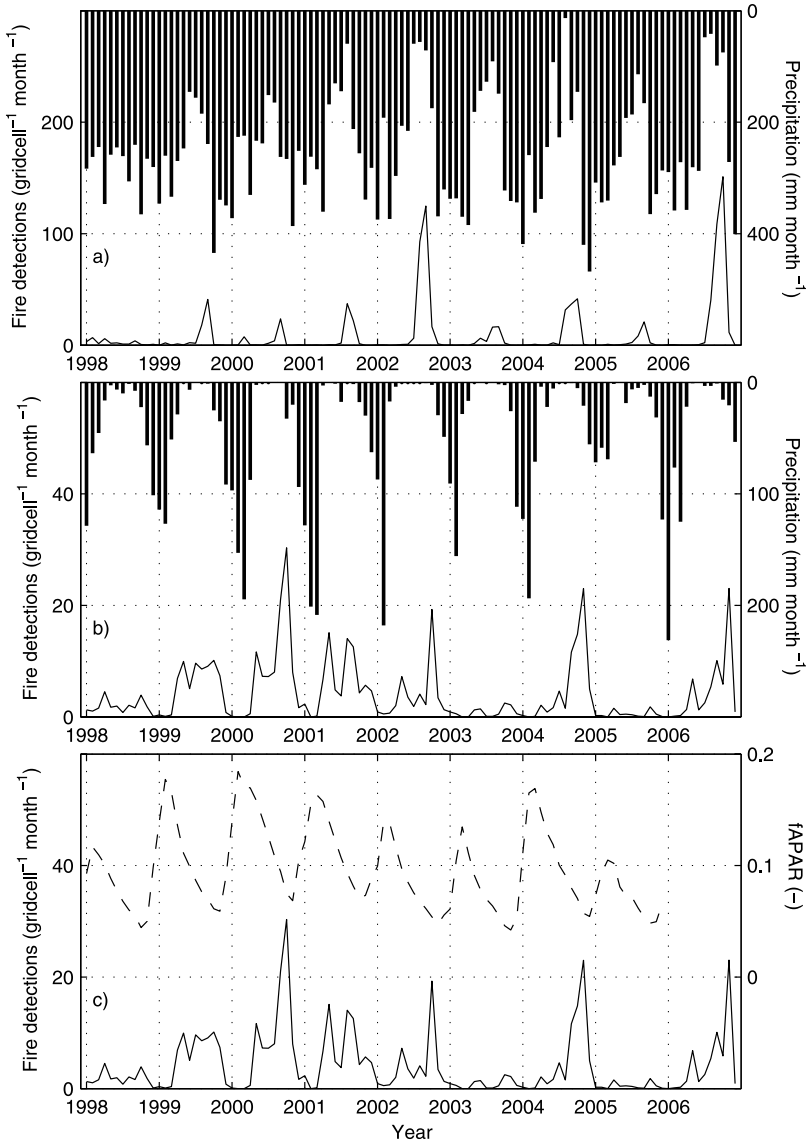

Figure 4. Time series of monthly precipitation and active fire detections for (a) a wet ecosystem (southern Borneo, latitude 2°S–4°S, longitude 110°E–116°E) where fire activity was higher during drought periods, (b) an arid ecosystem (northwest Australia, latitude 17°S–20°S, longitude 114°E–131°E) where fire activity was higher after a wet season with abundant rainfall, and (c) the same region as Figure 4b with average monthly fAPAR (not available for 2006) plotted instead of monthly precipitation.

bands, interannual variability in fire activity was often not related to climate indicating that other factors were equally important for explaining the spatial and interannual variability of fire activity here (see the discussion section).

[23] Africa had on average the highest burned fraction in these intermediate precipitation and productivity ecosystems, followed by Australia (Figures 5 and 6). It is important to note that the data plotted in Figures 5 and 6 were averaged over whole continents for the precipitation or NPP bins, and that variability between grid cells was large.

3.3. Arid Ecosystems

[24] At the low end of the precipitation range fire activity increased with increasing levels of precipitation or NPP (Figures 5 and 6). The relation between precipitation or NPP and burned fraction was often close to linear in these arid ecosystems, except in Africa where there seemed to be a threshold above which fires occurred that is higher than in other regions.

[25] Northern Australia provided the clearest example of the dependence of fire activity on climate in arid ecosystems, both spatially (Figures 1a and 1b) and temporally (Figures 3b, 4b, and 4c). In the interior where precipitation rates were low, fires were non-existent. Toward the northern coast, precipitation increases (Figure 1a) were linked with increases in both active fire (Figure 1a) and burned area (Figure 6d). The same gradient was observed in northern Africa, where no fires occurred in the Sahara but substantial

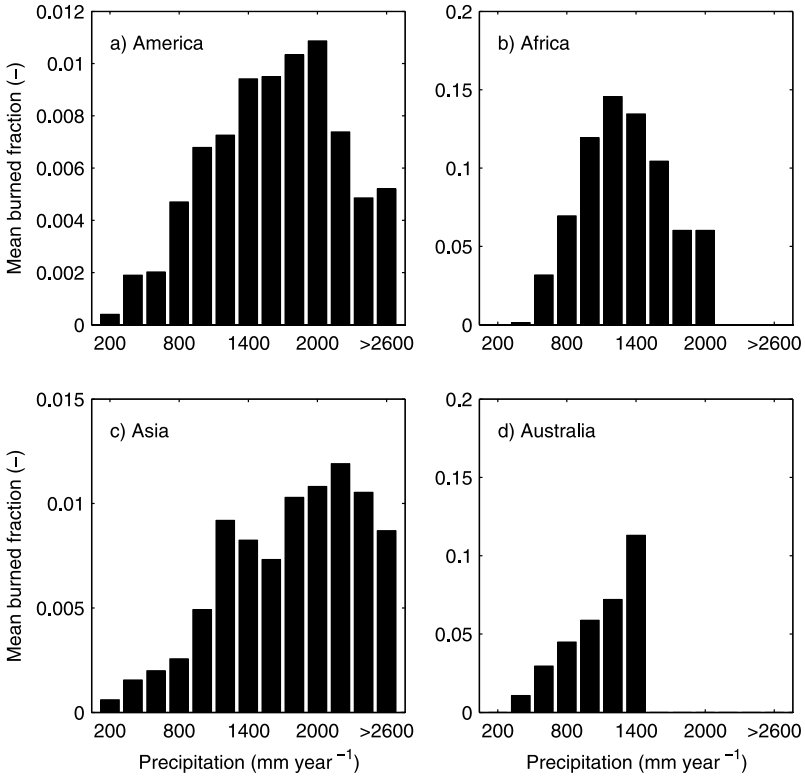

Figure 5. Mean burned fraction over a precipitation gradient for (a) North and South America between 38°N and 38°S, (b) Africa, (c) Asia south of 38°N, and (d) Australia. Values were averaged over 200-mm year^{-1} precipitation bins.

fire activity occurred in the Sahel. Moving into more productive ecosystems further south, the positive correlation between precipitation and active fire detections decreased.

3.4. Trends in Fire Activity

[26] Active fire detections decreased during 1998–2006 in all major biomass burning regions in the tropics and subtropics, except in the arc of deforestation and in Indonesia (Figure 8). This result did not change when we excluded 1998 (a high fire year) from the time series, although the decrease in eastern Borneo and Central America -both of which burned extensively in 1998- was smaller. In the arc of deforestation in the southern Amazon the northward movement of the fire front (toward the interior of the basin) is clearly visible. Due to high fuel loads, deforestation fires lead to a higher number of active fire detections per unit of burned area than fires in land uses that follow deforestation, such as agriculture or pasture [*van der Werf et al.*, 2003]. A clear deforestation front was not visible in the main deforestation regions in Indonesia (northeast Sumatra and southern Borneo), suggesting a more distributed pattern of development.

[27] In many savanna regions year-to-year variability was large and limited our ability to detect long-term trends. Especially in Australia where interannual variability was large the statistical significance was poor (Table 2). However, also in other regions significant decreasing trends (with p less than 0.05) was observed in only a small percentage of grid cells −14% for America, 17% for Africa, and 10% for Asia (Table 2). We did a similar trend analysis using ATSR active fire detections, which allowed for analysis of an 11 year period (July 1996–June 2007, not shown). This gave similar results with decreasing fire activity in savanna ecosystems in South America and Africa, but the decrease in Australia was not as widespread as when only taking the 1998–2006 or 1999–2006 period into account because of low fire activity in 1997. Within Africa, the trend was stronger and more robust in northern Africa than in southern Africa.

4. Discussion

4.1. Tropical Forest Ecosystems

[28] In wet tropical forest ecosystems the number of detected active fires was closely linked with the length and intensity of the dry season (Figure 9). Not all fires detected in this biome were necessarily deforestation fires; some fires may have resulted from pasture or agricultural waste burning in areas already deforested. For this study, however, we assumed that all or at least most of the fire detections were deforestation fires because they occurred in areas previously classified as tropical forest and because they are associated with the progressing fire front (Figure 8). Using higher resolution data, it may be possible in the future to more quantitatively partition active fire detections and burned area into deforestation and other land use activities.

[29] Interannual variability in climate was largest in Asia, having a marked impact on fire activity from year to year

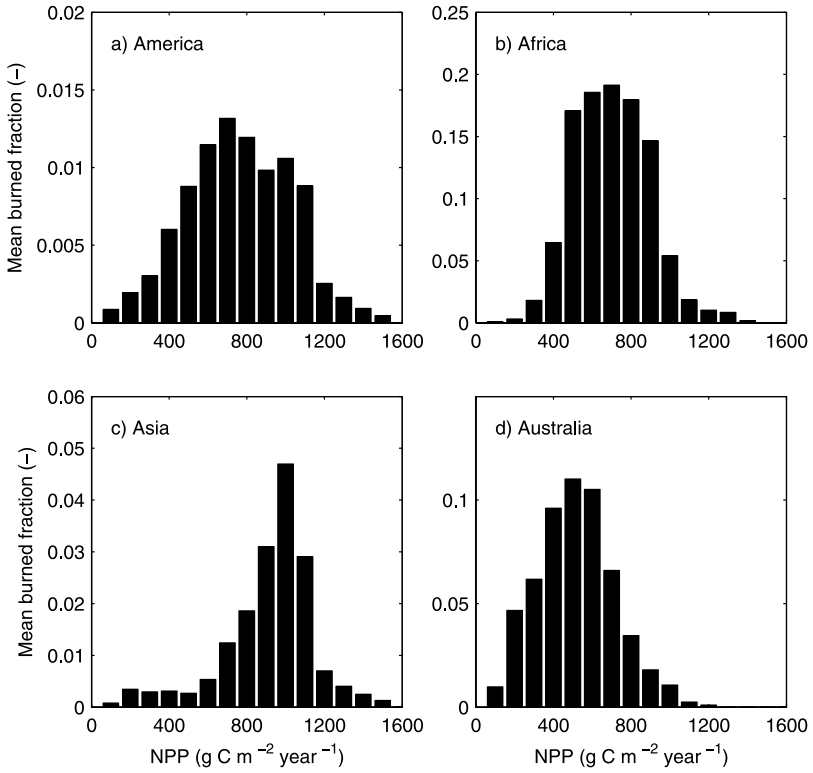

Figure 6. Mean burned fraction over a net primary production (NPP) gradient for (a) North and South America between 38°N and 38°S, (b) all of Africa, (c) Asia south of 38°N, and (d) Australia. Values were averaged over 100-g C m^2 $year^{-1}$ NPP bins.

(Figure 3a). Although in America and Africa the majority of the grid cells showed dependence of active fires on climate (Figure 3a), this relation was not as clear and uniform as in Asia with its larger interannual variability. Past work has shown that fire activity increases during drought years in specific regions undergoing deforestation [*Cardoso et al.*, 2003; *Nepstad et al.*, 2004]. Our results indicate, however, that the drought–fire relation is not uniform and is weaker in the Amazon and Africa than in Asia (Figure 3a). In the Amazon most fire-driven deforestation occurs in the southern part of the basin. Here, the relatively long dry season may never fully limit the use of fire, so that fires can be

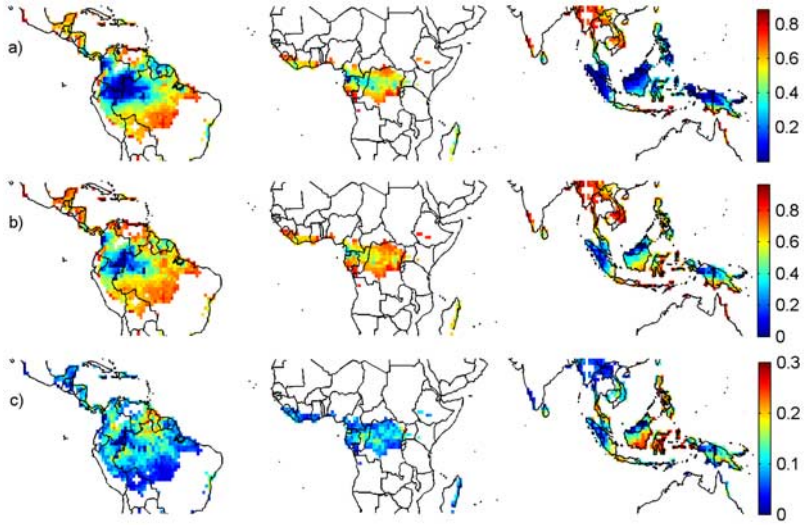

Figure 7. (a) Mean, (b) maximum, and (c) standard deviation of fire deforestation potential (FDP) for all tropical forest grid cells for 1998–2006. High FDP values indicate climate conditions suitable for the use of fire.

Table 1. Total Area (Million km^2) or Percentage of Tropical Forest Area Below FDP Thresholds for Tropical America, Africa, and Asia

FDP Threshold	Total Forest Area (M km^2)			Percent of Forest Area		
	America	Africa	Asia	America	Africa	Asia
<0.1	1.09	0.02	1.58	11	1	21
<0.2	1.73	0.10	2.58	18	3	34
<0.3	2.56	0.26	3.15	26	8	41
<0.4	3.32	0.56	3.66	34	18	48
<0.5	4.71	1.11	4.10	48	36	53
<0.6	6.74	1.97	4.47	69	64	58
<0.7	8.45	2.70	5.04	87	87	66
<0.8	9.21	3.05	5.69	95	98	74
<0.9	9.26	3.07	5.82	95	99	76
<=1.0	9.72	3.09	7.68	100	100	100

Table 2. Percentage of Grid Cells With an Increasing (Positive) or Decreasing (Negative) Trend[a]

Statistical Significance	America		Africa		Asia		Australia	
	+	–	+	–	+	–	+	–
All grid cells	33	67	22	78	42	58	25	75
Cells with $p < 0.05$	4	10	1	16	4	6	1	4

[a]Only grid cells with a slope greater than 5% per year were taken into account.

ignited each year. *Morton et al.* [2006] showed that the price of soy and deforestation rates was positively correlated in the state of Mato Grosso in the southern Amazon, suggesting that socio-economic factors play an important role in interannual variability of deforestation rates. On the basis of the results presented here, climate also drives interannual variability in deforestation rates, although more research is needed to quantify the relative importance of these two sets of drivers and interactions between them. The role of climate in determining variability in fire activity, however, may increase in the future in the southern Amazon as the deforestation front moves to regions which experience a shorter dry season (Figure 7a).

[30] Our results have several implications for future fire-driven deforestation rates. Projections of future deforestation are generally based on the construction of roads, population densities, and other socio-economic incentives [e.g., *Laurance et al.*, 2004]. However, if fire is used as a primary tool in the clearing process, then climate (and specifically the moisture balance of tropical forests) should also be included in these scenarios. Our FDP scalar provides a measure of the potential vulnerability of forests to human fire use, solely considering climate effects. The actual rate of deforestation will depend on many other factors in addition to climate, including nearby infrastructure, economic incentives, and changes in global markets [*Cardoso et al.*, 2003].

[31] If the deforestation front in the Amazon progresses further into the interior with time, the dry season will be shorter and fire will not be as useful as a tool in the land clearing process. This has the potential to limit rates of land clearing, although the importance of this limitation may vary regionally and will depend on the availability of mechanized equipment and access to international markets (and thus to variability in global commodity prices). Moreover, *Hoffmann et al.* [2003] showed that in most tropical forest areas future climate may increase fire risk because droughts may become more severe.

[32] Future fire conditions at the deforestation front thus depend partly on the balance between the pace of global and regional climate change and the speed of deforestation. In the Amazon, most models indicate reduced precipitation during the dry season [*Christensen et al.*, 2007; *Malhi et al.*, 2008] which would increase fire risk, although some models predict an increase in available moisture (precipitation minus evapotranspiration) in the future which has the potential to lower fire risk [*Held and Soden*, 2006]. Models predicting lower precipitation during the dry season show that the interior of the Amazon will be less impacted than the fringes; this indicates that areas having low FDP values now may continue to have low vulnerability during the remainder of the 21st century. Key to regional climate change may be the patchiness of deforestation; complete deforestation will lead to a stronger reduction in precipitation than if patches of forest remain [*Chagnon et al.*, 2004].

[33] The largest area of forest with low mean FDP values was in Asia. In Indonesia, FDP was generally low and periods with high fire activity coincided with El Niño periods. In this region, most of the variability occurred in the southern part of Borneo, which was severely impacted by ENSO and where widespread fires burned during 2002 and 2006. In the future, fire-driven deforestation rates here will be depend on how the ENSO regime changes. ENSO may intensify with climate warming, increasing fire vulnerability during the El Niño phase [*Li et al.*, 2007] although this is still a point of contention [*Christensen et al.*, 2007].

[34] Forests in the Congo basin had a greater vulnerability to fire use as compared with tropical forests in South America and Asia. In the Congo basin, however, fewer

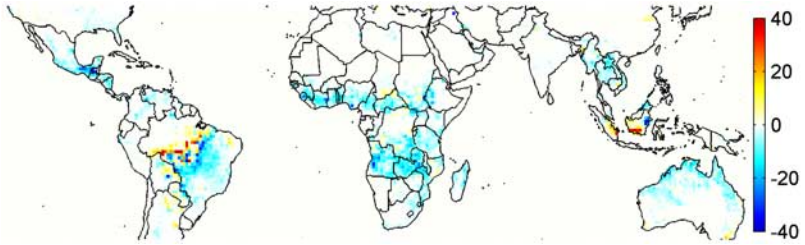

Figure 8. Linear trend of TRMM-VIRS active fire detections (active fire detections per year) during 1998–2006. Fire activity decreased in most savanna ecosystems in Central and South America, Africa, and Australia. The inward movement of the fire front is visible in the arc of deforestation in the Amazon, and fire activity has increased in deforestation regions in Indonesia.

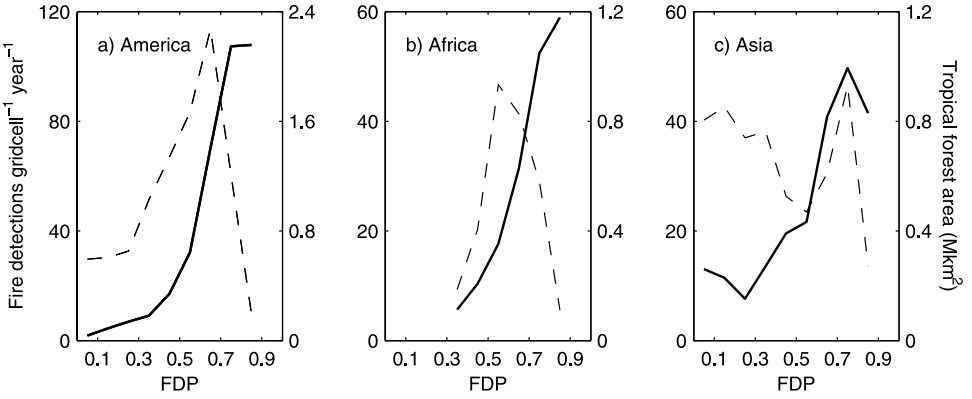

Figure 9. Observed TRMM-VIRS active fire detections as a function of FDP for all tropical forest grid cells in (a) tropical America, (b) Africa, and (c) Asia (solid lines). Dashed lines indicate the distribution of tropical forest area over FDP bins. Values were averaged over 0.1 FDP bins.

fires were observed in tropical forest areas as indicated by the number of fire detections per grid cell (Figure 9b), providing qualitative evidence for less fire-driven deforestation than in the Amazon.

4.2. Intermediate and Low Productivity Ecosystems

[35] Savanna ecosystems with intermediate levels of productivity had the highest fire frequency. During the annual prolonged dry season these ecosystems experience, herbaceous fuels dry out and the landscape becomes vulnerable to fire. Although our results clearly showed that these were the most frequently burning regions because they were neither limited by fuel loads nor by the length of the dry season, variability in this region could not be explained solely by variability in climate (Figures 5 and 6).

[36] In savanna ecosystems, the seasonal timing of ignition by humans probably varies with different land use and fire practices. Fires may be set late in the dry season to increase their intensity and effectiveness in removing shrubs and saplings. In contrast, fires may also be set in the beginning of the dry season to limit erosion and loss of soil nutrients [*Williams et al.*, 1998]. These different practices may contribute to the large spread and high standard deviations (usually exceeding the mean values plotted in Figures 5 and 6) we found in these intermediate productivity ecosystems. These intermediate ecosystems may also contain patches of intact forest as is the case, for example, in the southern Amazon. Here, economic and political incentives may be important drivers of interannual variability of fire activity (see above). In Africa where we found less fire in tropical forests than in the Amazon (Figure 9) and where the majority of the fires were detected in savanna areas, the relation between precipitation and active fire detections was less variable than in other regions. Here, when precipitation rates exceeded 1500 mm year^{-1} fire activity decreased substantially. This was less evident in America and Asia, where fires are used extensively in the deforestation process [*Morton et al.*, 2006; *Langner et al.*, 2007].

[37] Interactions between climate, grazing, agriculture, and fire are complex and can vary regionally with different patterns of land use. In northern Africa, for example, grid cells with a strong positive response between precipitation and fire activity were immediately adjacent to grid cells with a negative response, despite having similar climate and plant functional type distributions. In the more productive parts of these intermediate ecosystems, interannual variability in fire activity was partly linked to climate. In the woodlands in southern Africa fire activity increased during drought years (Figure 3a), probably because fires not only combusted the herbaceous layer but also shrubs and trees so that fuel loads depended less on precipitation rates during the preceding wet season.

[38] In semi-arid ecosystems, the underlying mechanisms for the strong positive correlation between precipitation and fire activity are not fully understood. Many of these areas experience intensive grazing, including northern Australia [*Fensham et al.*, 1999]. An important question for future research is to identify the degree to which land managers in arid ecosystems modify ignition patterns in response to drought. In the absence of year-to-year differences in ignition, greater herbaceous fuel accumulation during wet years may allow for larger fire sizes and more burned area during the following dry season [*Griffin et al.*, 1983; *Swetnam and Betancourt*, 1990; *van Wilgen et al.*, 2000]. An alternative explanation, however, is that land managers ignite more fires during wet years than during dry years. This could occur for several reasons; setting fewer fires during dry years for example may preserve a larger fraction of the remaining aboveground biomass as forage for livestock and wild game. Igniting more fires during wet years (when there is an excess of forage for livestock) may be part of a broader strategy to avoid woody encroachment within grasslands.

[39] Representing fire dynamics in tropical ecosystems with intermediate productivity in land use models or DGVM's may be challenging because of the multiple ways humans use fire in land management. In these areas, human decisions on whether and when to use fire may change seasonally and regionally–influencing interactions with climate. In arid and high productivity ecosystems, human regulation of the fire regime is probably no less important, but the role of climate may be more easily represented in climate-carbon models. Our quantitative assessment indicated that climate is a main controlling factor of fire processes in these two extreme ecosystems, although also

here variations occur spatially and regionally, indicating that other factors besides climate are important to include in fire models aiming to better understand the role of fire under future climate conditions.

[40] The decreases in active fire detections over 1998–2006 coincided with decreasing precipitation rates in fuel limited areas (northern Africa, Australia) and increasing precipitation rates in several areas which normally burn more extensively during drought periods (most notably the southern Africa woodlands). The increasing trend in southern Borneo was the result of the relatively short time period considered here, with La Niña conditions in 1999 and 2000 and a weak and moderate El Niño in 2002 and 2006.

4.3. Uncertainties

[41] The satellite record showed that although climate limits fire activity at the extreme ends of the precipitation range, it can account for only part of the observed spatial and temporal variability of fires in ecosystems with intermediate levels of productivity. The standard deviations of the values plotted in Figures 5 and 6 usually exceeded the absolute value, and our conclusions are most robust when averaging observations at a regional or continental scale. In the grid-by-grid analyses, many cells did not show a significant relationship between climate and fire in intermediate productivity ecosystems. This indicates that, although climate plays an important role in providing boundary conditions for fires, there is a relatively large range of climate conditions for which other factors including vegetation type, grazing, agriculture, and fire management are equally or more important in explaining observed patterns.

[42] Active fire detection algorithms primarily rely on observations in the visible and infrared part of the electromagnetic spectrum and therefore cannot detect fires during periods of abundant, optically thick cloud cover [*Schroeder et al.*, 2008]. This may partly contribute to the observed decline in active fire detections in areas with high PPT (and thus clouds). The TRMM-VIRS fire data, however, are adjusted for this effect via a correction factor derived from the monthly mean cloud fraction [*Giglio et al.*, 2003]. Future analyses could further circumvent this issue using new, multi-year burned area data sets which have recently become available [*Roy et al.*, 2005; *Tansey et al.*, 2008] and which are not partly based on active fire observations as is the case with the burned area product used here.

[43] We performed a similar analysis using ATSR night time fires [*Arino et al.*, 1999]. This somewhat strengthened the drought-fire link in high productivity tropical forest ecosystems, with in general lower *p*-values than when using TRMM-VIRS derived fire activity (not shown). Fire activity peaks during the mid to late afternoon because of lower humidity, increased wind speeds, and higher human activity [*Giglio*, 2007]. Several classes of fire that occur during the day may have weaker climate regulation than fires that persist over a full diurnal cycle. Agricultural waste burning, for example, will mostly take place during daytime and may not be detected by ATSR. This contrasts with forest fires that are likely to burn in many places during day and night for a period of days to weeks. We choose to base our analysis on TRMM-VIRS because our main climatic factor -precipitation- was also derived from the TRMM satellite and because including the whole diurnal cycle may give a more complete representation of fire activity. The trade off is a shorter time series; ATSR currently provides the longest continuous fire record starting mid 1996 against 1998 for TRMM-VIRS.

[44] Finally, we assumed that fire activity depended on drought defined solely by PPT anomalies during the same dry season, or alternately, fuel build-up defined solely by PPT anomalies during preceding wet season. As a consequence, multi-year effects were not captured by our approach. One example is the positive feedback which has been reported for closed canopy forests, where fires lead to higher fuel loads and to an opening of the canopy which increases the susceptibility of the forests to fire [*Cochrane et al.*, 1999; *Nepstad et al.*, 1999]. Another example may be that in arid regions, two consecutive years with intermediate rainfall rates may provide fuel loads similar to one wet year, leading to similar fuel conditions under different climatic conditions. Some of these processes also operate on finer resolutions than our 1° analysis, and further investigation is needed to better understand these more complex interactions between fire processes, climate, and fire activity.

5. Conclusions

[45] We used satellite observations of precipitation (PPT), fAPAR, and fire activity during 1998–2006 in the tropics and subtropics to study climatic controls on fire activity. Although fire has largely become a human-driven phenomenon in the tropics and subtropics, we found that because climate regulates the amount of dry fuel available for ignition, it has a strong impact on the spatial and interannual variability of fire activity. In arid regions, fire activity was limited by the density of available fuels, governed largely by the amount of precipitation during the preceding wet season. In wet ecosystems, fires occurred in years that had extended dry seasons, allowing fuels to dry out. Fire frequencies were highest in savanna ecosystems with intermediate levels of productivity (net primary production between 500–1000 g C m^{-2} $year^{-1}$).

[46] We found that the highest interannual variability in fire activity occurred in Indonesia and northern Australia where climate and PPT were closely tied to ENSO. During El Niño periods, drought in forested regions in Indonesia allowed humans to use fire more effectively and led to an increase of active fire detections. At the same time drought lowered the number of active fire detections in arid regions in Australia. The decrease in Australian fires may have been caused by lower fuel loads (and thus smaller fires) and by the decision by land managers to set fewer fires to preserve forage for grazing by livestock.

[47] In tropical forests in the Amazon and Congo basins, spatial variability in precipitation rates and fires were closely linked but interannual variability in precipitation rates was not as large as in Indonesia. Interannual variability in fire activity was also lower and correlations between climate and fire were not as uniform over the region as in Indonesia. A large part of the deforestation takes place in the southern part of the Amazon where the dry season is much longer than in Indonesia. Therefore other (socio-economic) factors may be

equally important in driving interannual variability. In the future, however, the gradient toward increasing precipitation in the interior of the forest may slow fire-driven deforestation. Future deforestation projections should take this negative feedback into account, although its effect may be limited as several climate models have indicated a decrease in precipitation over the Amazon due to global and regional climate change, the latter partly depending on the effects of deforestation on surface biophysical properties.

[48] **Acknowledgments.** We thank G. J. Collatz for valuable comments and R. S. DeFries and D. C. Morton for sharing insights in fire dynamics in deforestation regions. G.R.v.d.W. was supported by a Veni grant from the Netherlands Organization for Scientific Research, J.T.R. was supported by NASA grant NNG04GK49G, and L.G. was supported by NSF grant 0628353. All data used to construct the graphs can be downloaded from http://www.geo.vu.nl/~gwerf/pubs/2008GBCfirecontrols.

References

Arino, O., J.-M. Rosaz, and P. Goloub (1999), The ATSR World Fire Atlas: A synergy with "Polder" aerosol products, *Earth Obs. Quarterly*, *64*, 1–6.

Barbosa, P. M., D. Stroppiana, J. M. Gregoire, and J. M. C. Pereira (1999), An assessment of vegetation fire in Africa (1981–1991): Burned areas, burned biomass, and atmospheric emissions, *Global Biogeochem. Cycles*, *13*(4), 933–950.

Bishop, J. K. B., and W. B. Rossow (1991), Spatial and temporal variability of global surface solar irradiance, *J. Geophys. Res.*, *96*(C9), 16,839–16,858.

Bond, W. J., F. I. Woodward, and G. F. Midgley (2005), The global distribution of ecosystems in a world without fire, *New Phytol.*, *165*(2), 525–537.

Cahoon, D. R., B. J. Stocks, J. S. Levine, W. R. Cofer, and K. P. Oneill (1992), Seasonal distribution of African savanna fires, *Nature*, *359*(6398), 812–815.

Cardoso, M. F., G. C. Hurtt, B. Moore, C. A. Nobre, and E. M. Prins (2003), Projecting future fire activity in Amazonia, *Glob. Chang. Biol.*, *9*(5), 656–669.

Chagnon, F. J. F., R. L. Bras, and J. Wang (2004), Climatic shift in patterns of shallow clouds over the Amazon, *Geophys. Res. Lett.*, *31*(24), L24212, doi:10.1029/2004GL021188.

Christensen, J., et al. (2007), Regional climate projections, in *Climate Change 2007: The Physical Science Basis. Contribution of Working Group I to the Fourth Assessment Report of the Intergovernmental Panel on Climate Change*, edited by S. Solomon et al., Cambridge Univ. Press, New York.

Cochrane, M. A. (2003), Fire science for rainforests, *Nature*, *421*(6926), 913–919.

Cochrane, M. A., A. Alencar, M. D. Schulze, C. M. Souza, D. C. Nepstad, P. Lefebvre, and E. A. Davidson (1999), Positive feedbacks in the fire dynamic of closed canopy tropical forests, *Science*, *284*(5421), 1832–1835.

Curran, L. M., S. N. Trigg, A. K. McDonald, D. Astiani, Y. M. Hardiono, P. Siregar, I. Caniago, and E. Kasischke (2004), Lowland forest loss in protected areas of Indonesian Borneo, *Science*, *303*(5660), 1000–1003.

Dozier, J. (1981), A method for satellite identification of surface-temperature fields of subpixel resolution, *Remote Sens. Environ.*, *11*(3), 221–229.

Fensham, R. J., J. E. Holman, and M. J. Cox (1999), Plant species responses along a grazing disturbance gradient in Australian grassland, *J. Veg. Sci.*, *10*(1), 77–86.

Field, C. B., M. J. Behrenfeld, J. T. Randerson, and P. Falkowski (1998), Primary production of the biosphere: Integrating terrestrial and oceanic components, *Science*, *281*(5374), 237–240.

Forster, P., et al. (2007), Changes in atmospheric constituents and in radiative forcing, in *Climate Change 2007: The Physical Science Basis. Contribution of Working Group I to the Fourth Assessment Report of the Intergovernmental Panel on Climate Change*, edited by S. Solomon et al., Cambridge Univ. Press, New York.

Friedl, M. A., et al. (2002), Global land cover mapping from MODIS: Algorithms and early results, *Remote Sens. Environ.*, *83*(1–2), 287–302.

Giglio, L. (2007), Characterization of the tropical diurnal fire cycle using VIRS and MODIS observations, *Remote Sens. Environ.*, *108*(4), 407–421.

Giglio, L., G. R. van der Werf, J. T. Randerson, G. J. Collatz, and P. Kasibhatla (2006), Global estimation of burned area using MODIS active fire observations, *Atmos. Chem. Phys.*, *6*, 957–974.

Giglio, L., J. D. Kendall, and R. Mack (2003), A multi-year active fire data set for the tropics derived from the TRMM VIRS, *Int. J. Remote Sens.*, *24*(22), 4505–4525.

Gobron, N., B. Pinty, F. Melin, M. Taberner, and M. M. Verstraete (2002), *Sea Wide Field-of-View Sensor (SeaWiFS)—an optimized FAPAR Algorithm Theoretical Basis Document*, Institute for Environment and Sustainability, Joint Research Center, Ispra, Italy. (JRC Publication No. EUR 20148 EN)

Gobron, N., et al. (2006), Evaluation of fraction of absorbed photosynthetically active radiation products for different canopy radiation transfer regimes: Methodology and results using Joint Research Center products derived from SeaWiFS against ground-based estimations, *J. Geophys. Res.*, *111*(D13), D13110, doi:10.1029/2005JD006511.

Goldammer, J. G. (1990), *Fire in the Tropical Biota. Ecosystem Processes and Global Challenges*, 497 pp., Springer, New York.

Grégoire, J. M., K. Tansey, and J. M. N. Silva (2003), The GBA2000 initiative: Developing a global burnt area database from SPOT-VEGETATION imagery, *Int. J. Remote Sens.*, *24*(6), 1369–1376.

Griffin, G. F., N. F. Price, and H. F. Portlock (1983), Wildfires in the Central Australian Rangelands, 1970–1980, *J. Environ. Manag.*, *17*(4), 311–323.

Hansen, J., R. Ruedy, J. Glascoe, and M. Sato (1999), GISS analysis of surface temperature change, *J. Geophys. Res.*, *104*(D24), 30,997–31,022.

Held, I. M., and B. J. Soden (2006), Robust responses of the hydrological cycle to global warming, *J. Clim.*, *19*(21), 5686–5699.

Hoffmann, W. A., W. Schroeder, and R. B. Jackson (2003), Regional feedbacks among fire, climate, and tropical deforestation, *J. Geophys. Res.*, *108*(D23), 4721, doi:10.1029/2003JD003494.

Huffman, G. J., R. F. Adler, B. Rudolf, U. Schneider, and P. R. Keehn (1995), Global precipitation estimates based on a technique for combining satellite-based estimates, rain-gauge analysis, and NWP model precipitation information, *J. Clim.*, *8*(5), 1284–1295.

Kummerow, C., W. Barnes, T. Kozu, J. Shiue, and J. Simpson (1998), The Tropical Rainfall Measuring Mission (TRMM) sensor package, *J. Atmos. Ocean. Technol.*, *15*(3), 809–817.

Langner, A., J. Miettinen, and F. Siegert (2007), Land cover change 2002–2005 in Borneo and the role of fire derived from MODIS imagery, *Glob. Chang. Biol.*, *13*(11), 2329–2340, doi:10.1111/j.1365-2486.2007.01442.x.

Laurance, W. F., A. K. M. Albernaz, P. M. Fearnside, H. L. Vasconcelos, and L. V. Ferreira (2004), Deforestation in Amazonia, *Science*, *304*(5674), 1109–1111.

Li, W. H., R. E. Dickinson, R. Fu, G. Y. Niu, Z. L. Yang, and J. G. Canadell (2007), Future precipitation changes and their implications for tropical peatlands, *Geophys. Res. Lett.*, *34*(1), L01403, doi:10.1029/2006GL028364.

Malhi, Y., J. T. Roberts, R. A. Betts, T. J. Killeen, W. H. Li, and C. A. Nobre (2008), Climate change, deforestation, and the fate of the Amazon, *Science*, *319*(5860), 169–172.

Morton, D. C., R. S. DeFries, Y. E. Shimabukuro, L. O. Anderson, E. Arai, F. D. Espirito-Santo, R. Freitas, and J. Morisette (2006), Cropland expansion changes deforestation dynamics in the southern Brazilian Amazon, *Proc. Natl. Acad. Sci. U.S.A.*, *103*(39), doi:10.1073/pnas.0606377103.

Murdiyarso, D., L. Lebel, A. N. Gintings, S. M. H. Tampubolon, A. Heil, and M. Wasson (2004), Policy responses to complex environmental problems: insights from a science-policy activity on transboundary haze from vegetation fires in Southeast Asia, *Agric., Ecosyst. Environ.*, *104*(1), 47–56.

Negri, A. J., T. L. Bell, and L. M. Xu (2002), Sampling of the diurnal cycle of precipitation using TRMM, *J. Atmos. Ocean. Technol.*, *19*(9), 1333–1344.

Nepstad, D., P. Lefebvre, U. L. Da Silva, J. Tomasella, P. Schlesinger, L. Solorzano, P. Moutinho, D. Ray, and J. G. Benito (2004), Amazon drought and its implications for forest flammability and tree growth: A basin-wide analysis, *Glob. Chang. Biol.*, *10*(5), 704–717.

Nepstad, D. C., et al. (1999), Large-scale impoverishment of Amazonian forests by logging and fire, *Nature*, *398*(6727), 505–508.

New, M., M. Hulme, and P. Jones (1999), Representing twentieth-century space-time climate variability. Part I: Development of a 1961–90 mean monthly terrestrial climatology, *J. Clim.*, *12*(3), 829–856.

Page, S. E., F. Siegert, J. O. Rieley, H. D. V. Boehm, A. Jaya, and S. Limin (2002), The amount of carbon released from peat and forest fires in Indonesia during 1997, *Nature*, *420*(6911), 61–65.

Phillips, O. L. (1997), The changing ecology of tropical forests, *Biodivers. Conserv.*, *6*(2), 291–311.

Phillips, O. L., P. Hall, A. H. Gentry, S. A. Sawyer, and R. Vasquez (1994), Dynamics and species richness of tropical rain-forests, *Proc. Natl. Acad. Sci. U.S.A.*, *91*(7), 2805–2809.

Potter, C. S., J. T. Randerson, C. B. Field, P. A. Matson, P. M. Vitousek, H. A. Mooney, and S. A. Klooster (1993), Terrestrial ecosystem production—A process model-based on global satellite and surface data, *Global Biogeochem. Cycles*, *7*(4), 811–841.

Prins, E. M., and W. P. Menzel (1992), Geostationary satellite detection of biomass burning in South-America, *Int. J. Remote Sens.*, *13*(15), 2783–2799.

Randerson, J. T., G. R. van der Werf, G. J. Collatz, L. Giglio, C. J. Still, P. Kasibhatla, J. B. Miller, J. W. C. White, R. S. DeFries, and E. S. Kasischke (2005), Fire emissions from C3 and C4 vegetation and their influence on interannual variability of atmospheric CO_2 and $\delta^{13}CO_2$, *Global Biogeochem. Cycles*, *19*, GB2019, doi:10.1029/2004GB002366.

Ropelewski, C. F., and M. S. Halpert (1987), Global and regional scale precipitation patterns associated with the El-Nino Southern Oscillation, *Mon. Weather Rev.*, *115*(8), 1606–1626.

Roy, D. P., Y. Jin, P. E. Lewis, and C. O. Justice (2005), Prototyping a global algorithm for systematic fire-affected area mapping using MODIS time series data, *Remote Sens. Environ.*, *97*(2), 137–162.

Saleska, S. R., et al. (2003), Carbon in amazon forests: Unexpected seasonal fluxes and disturbance-induced losses, *Science*, *302*(5650), 1554–1557.

Scholes, R. J., and S. R. Archer (1997), Tree-grass interactions in savannas, *Annu. Rev. Ecol. Syst.*, *28*, 517–544.

Schroeder, W., I. Csiszar, and J. Morisette (2008), Quantifying the impact of cloud obscuration on remote sensing of active fires in the Brazilian Amazon, *Remote Sens. Environ.*, *112*(2), 456–470.

Siegert, F., G. Ruecker, A. Hinrichs, and A. A. Hoffmann (2001), Increased damage from fires in logged forests during droughts caused by El Nino, *Nature*, *414*(6862), 437–440.

Spessa, A., B. McBeth, and C. Prentice (2005), Relationships among fire frequency, rainfall and vegetation patterns in the wet-dry tropics of northern Australia: An analysis based on NOAA-AVHRR data, *Glob. Ecol. Biogeogr.*, *14*(5), 439–454.

Stroppiana, D., S. Pinnock, and J. M. Gregoire (2000), The global fire product: Daily fire occurrence from April 1992 to December 1993 derived from NOAA AVHRR data, *Int. J. Remote Sens.*, *21*(6–7), 1279–1288.

Swetnam, T. W., and J. L. Betancourt (1990), Fire-southern oscillation relations in the southwestern United States, *Science*, *249*(4972), 1017–1020.

Tansey, K., et al. (2004), Vegetation burning in the year 2000: Global burned area estimates from SPOT VEGETATION data, *J. Geophys. Res.*, *109*(D14), D14S03, doi:10.1029/2003JD003598.

Tansey, K., J. M. Grégoire, P. Defourny, R. Leigh, J. F. O. Pekel, E. van Bogaert, and E. Bartholome (2008), A new, global, multi-annual (2000–2007) burnt area product at 1 km resolution, *Geophys. Res. Lett.*, *35*(1), L01401, doi:10.1029/2007GL031567.

van der Werf, G. R., J. T. Randerson, G. J. Collatz, and L. Giglio (2003), Carbon emissions from fires in tropical and subtropical ecosystems, *Glob. Chang. Biol.*, *9*(4), 547–562.

van der Werf, G. R., J. T. Randerson, G. J. Collatz, L. Giglio, P. S. Kasibhatla, A. F. Arellano, S. C. Olsen, and E. S. Kasischke (2004), Continental-scale partitioning of fire emissions during the 1997 to 2001 El Nino/La Nina period, *Science*, *303*(5654), 73–76.

van der Werf, G. R., J. T. Randerson, L. Giglio, G. J. Collatz, P. S. Kasibhatla, and A. F. Arellano (2006), Interannual variability in global biomass burning emissions from 1997 to 2004, *Atmos. Chem. Phys.*, *6*, 3423–3441.

van Langevelde, F., et al. (2003), Effects of fire and herbivory on the stability of savanna ecosystems, *Ecology*, *84*(2), 337–350.

van Wilgen, B. W., H. C. Biggs, S. P. O'Regan, and N. Mare (2000), A fire history of the savanna ecosystems in the Kruger National Park, South Africa, between 1941 and 1996, *S. Afr. J. Sci.*, *96*(4), 167–178.

Williams, R. J., A. M. Gill, and P. H. R. Moore (1998), Seasonal changes in fire behaviour in a tropical Savanna in Northern Australia, *Int. J. Wildland Fire*, *8*(4), 227–239.

Yevich, R., and J. A. Logan (2003), An assessment of biofuel use and burning of agricultural waste in the developing world, *Global Biogeochem. Cycles*, *17*(4), 1095, doi:10.1029/2002GB001952.

A. J. Dolman and G. R. van der Werf, Department of Hydrology and Geo-Environmental Sciences, Faculty of Earth and Life Sciences, VU University Amsterdam, De Boelelaan 1085, 1081HV Amsterdam, Netherlands. (guido.van.der.werf@falw.vu.nl)

L. Giglio, Science Systems and Applications, Inc., 10210 Greenbelt Road, Suite 600, Lanham, MD 20706, USA.

N. Gobron, Global Environmental Monitoring Unit, Institute for Environment and Sustainability, European Commission Joint Research Centre, TP 440, Via Enrico Fermi 2749, I-21027 Ispra (VA), Italy.

J. T. Randerson, Department of Earth System Science, 3212 Croul Hall, University of California, Irvine, Irvine, CA 92697, USA.